World Conference on Social Sciences, Law and Public Policy
Hosted Online from Toronto, Canada
Date: 26th June 2026
Website: https://econferencia.com

TRANSFORMER-BASED RESONANT TRANSDUCERS FOR MOTION PARAMETER MEASUREMENT

Mukhtorov U. B.
Tashkent State Transport University,
1 Temiryulchilar Street, Tashkent 100167, Uzbekistan.

Abstract

This paper investigates the structural features of an existing transformer-based resonant transducer for motion parameter measurement and a newly developed transformer-based resonant transducer, and develops mathematical models for analyzing their principal performance characteristics. A comparative analysis of the derived expressions for the output signals and sensitivities of the existing and proposed transformer-based resonant transducers demonstrates that the sensitivity of the proposed transducer is w_m times higher than that of the existing one, where w_m is the number of turns of the multi-turn magnetic core. This improvement is achieved by designing each magnetic field source as a multi-turn magnetic core incorporating a section of the excitation winding, whose turns enclose all turns of the multi-turn magnetic core. Furthermore, the proposed transducer provides higher accuracy in measuring the velocity of the moving excitation winding (the monitored object) owing to the substantial reduction of the alternating component of the output signal that is not proportional to the velocity of motion. This improvement is achieved by taking the output signal, proportional to the linear velocity of the moving measuring winding, from the load terminals connected to the moving measuring winding tuned to the voltage resonance condition.

Keywords: transformer-based resonant motion parameter transducer, linear displacement, linear velocity, voltage resonance, magnetic flux, magnetomotive force (MMF), magnetic permeance, transformer, moving measuring winding, induced electromotive force (EMF), sensitivity.

Introduction

The automation of a wide range of technological processes relies on the use of primary transducers, which enable labor-intensive operations to be performed efficiently, reduce energy consumption, lower production costs, and improve product quality by maintaining operating conditions close to the optimum under both normal and emergency conditions [1–4]. However, one of the major obstacles to achieving these objectives is the lack of reliable motion parameter transducers (MPTs) capable of measuring displacement, velocity, acceleration, vibration, and other motion-related quantities under harsh operating conditions characterized by high dust concentration, humidity, and significant temperature variations.

A comparative analysis of the principal characteristics of existing motion parameter transducers shows that transformer-based motion parameter transducers represent one of the most promising solutions for improving the efficiency of modern monitoring and control systems. Owing to their high reliability, stable performance under severe operating conditions, and relatively high output power, these transducers satisfy the requirements of contemporary control and automation systems more effectively than other transducer types [3–5]. Nevertheless, the existing transformer-based transducers designed for measuring linear displacement and velocity exhibit several significant drawbacks, including non-uniform sensitivity over the entire measurement range and nonlinear static characteristics [5–8]. These limitations reduce the accuracy

of monitoring and control systems and, in some applications, decrease system stability margins. Consequently, the development of new transformer-based resonant motion parameter transducers capable of simultaneously measuring linear displacement and linear velocity with improved metrological and performance characteristics remains an important and relevant research problem.
To evaluate the technical capabilities of existing designs, the well-known transformer-based resonant motion parameter transducer (TRMPT) proposed in [9] for the simultaneous measurement of linear displacement and linear velocity is analyzed. Its structural configuration and the corresponding notation are shown in Fig. 1.
The transducer consists of an E-shaped magnetic core (1), whose base incorporates two permanent magnets (2) with oppositely oriented poles, producing magnetic fluxes that are summed in the central limb. A stationary concentrated excitation winding (3), supplied from an AC voltage source (typically sinusoidal), is wound around the central limb of the magnetic core. A movable concentrated measuring winding (4) is connected in series with a capacitor (5) and the primary winding of a transformer (6). The permanent magnets generate a constant magnetic flux between the parallel limbs of the magnetic core, whereas the excitation winding produces an alternating magnetic flux in the same region. Neglecting the active and reactive magnetic reluctances of the magnetic core, the magnetic field within the working air gap may be considered uniform.
The magnetic flux in the central limb is determined as follows:

$$\Phi_w = \Phi_{w.0} + \Phi_{w.m} sin(\omega t + \varphi_e), \qquad (1)$$

here $\Phi_{w.0} = 2F_{e.0.}G_{\mu wg}x = F_{e.0.}\mu_0 \frac{bx}{\delta_w}$; $\Phi_{w.m} = 2F_{e.m.}G_{\mu wg}x = F_{e.m.}\mu_0 \frac{bx}{\delta_w} \cdot sin(\omega t + \varphi_e)$ – the constant and alternating components of the working magnetic flux in the central elongated limb;

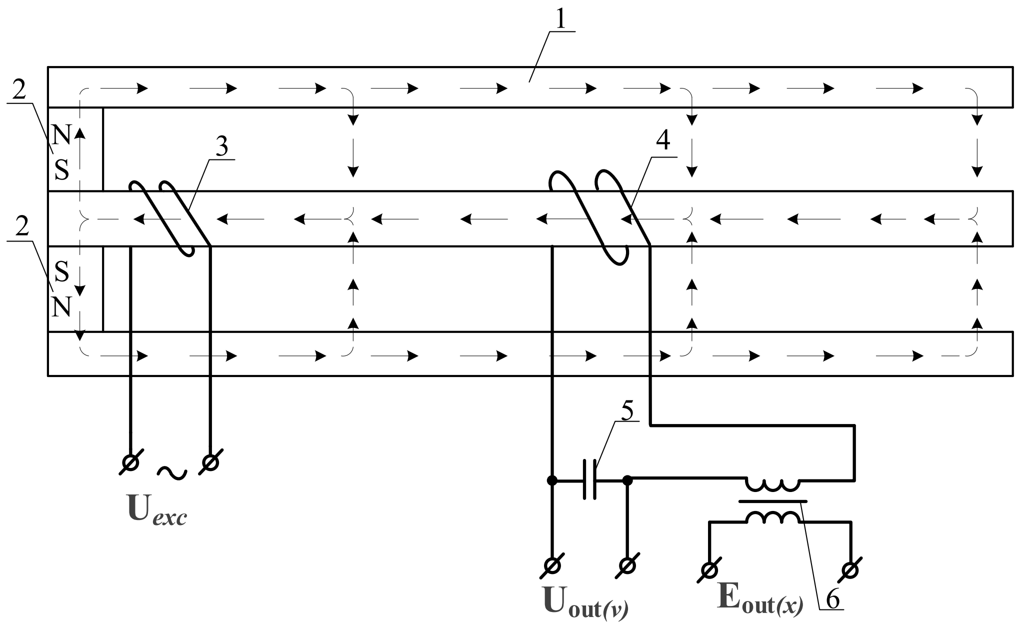

Fig. 1. Structural diagram of the existing motion parameter transducer.

$F_{e.0.}$ – magnetomotive force (MMF) of the permanent magnet; $F_{e.m.} = w_0 I_{e.m} sin(\omega t + \varphi_e)$ – the magnetomotive force (MMF) produced by the sinusoidal current in the excitation winding.; $I_{e.m}$, ω, φ_e – the amplitude, angular frequency, and initial phase of the sinusoidal current, respectively; w_0 – the number of turns in the excitation winding; $G_{\mu wg} = \mu_0 \frac{b}{\delta_w}$ – the per-unit-length magnetic permeance of the working air gap between two adjacent parallel elongated limbs; b , X_{M} and δ_w – the width, the length of the working section of the elongated limbs, and the working air gap between two adjacent limbs, respectively; μ_0 – the magnetic constant (the absolute permeability of free space); x – the coordinate of the moving measuring winding measured from the free ends of the elongated limbs.

As the moving measuring winding (4) moves, an electromotive force (EMF) is induced in it in accordance with the law of electromagnetic induction and is determined by the following expression:

$$e_{meas} = w_{meas}\frac{d\Phi_w}{dt} = E_v + e_x + e_{gen.} = 2w_{meas.}F_{e.0}G_{\mu wg}v +$$

$$+2\omega w_0 w_{mea.}I_{e.m}G_{\mu wg}x\cos(\omega t + \varphi_e) + 2w_0 w_{me..}I_{e.m}G_{\mu wg}v\sin(\omega t + \varphi_e), \quad (2)$$

here $E_v = 2w_{meas.}F_{e.0}G_{\mu wg}v$ – the constant component of the EMF proportional to the velocity of the moving winding; $e_x = 2\omega w_0 w_{meas.}I_{e.m}G_{\mu wg}x\cos(\omega t + \varphi_e)$ and $e_{gen.} = 2w_0 w_{meas.}I_{e.m}G_{\mu wg}v\sin(\omega t + \varphi_e)$ – the transformer component (proportional to the displacement of the moving winding) and the generator component (parasitic), respectively. $v = \frac{dx}{dt}$ – the linear velocity of the moving winding. It should be noted that the component $e_{gen.}$ is the source of the dynamic measurement error in displacement measurement.

The EMF component proportional to the displacement of the moving winding and taken from the secondary winding of transformer (6) can be expressed in complex form for $v = 0$ (Fig. 1) as follows:

$$\dot{E}_{out.(x)} = j2\sqrt{2}\omega w_0 w_{meas.}I_e G_{\mu wg}x. \quad (3)$$

The load current, according to the equivalent circuit (Fig. 2), is determined as follows:

$$\dot{I}_l = \frac{\dot{E}_{meas}}{R_{L.meas} + R_{L_1(tr)} + jX_{L.meas} + j(X_{L_1(tr)} - X_C)}, \quad (4)$$

here $R_{L.meas}$, $R_{L_1(tr)}$, $X_{L.meas}$, $X_{L_1(tr)}$ –the resistance and inductive reactance of the moving measuring winding (4) and the primary winding of transformer (6), respectively; X_C – the capacitive reactance of the capacitor.

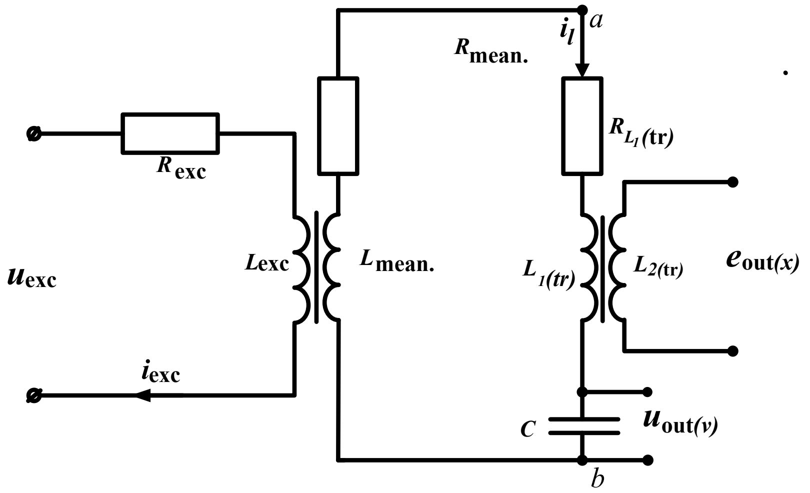

Fig. 2. Equivalent circuit of the existing motion parameter transducer.

The output voltage proportional to the velocity of the moving winding and taken from capacitor (5) is determined as the voltage drop across the capacitor's capacitive reactance, i.e.:

$$\dot{U}_{out.(v)} = E_v + j\dot{I}_{\text{н}}X_C. \quad (5)$$

The displacement sensitivity of the existing motion parameter transducer is determined as follows:

$$S_{prop.(x)} = \frac{dE_{out.(x)}}{dx}, \quad (6)$$

Now, let us determine the output signals and sensitivity of the existing motion parameter transducer using the following parameters: the geometric dimensions of the magnetic core and the numbers of turns of the transducer windings: $X_{\text{м}} = 0{,}1\ m$; $b = 0{,}02\ m$; $h = 0{,}01\ m$; $\delta_w = 0{,}01\ m$; $F_{e.0} = 100$ A; $w_{meas} =$ 10 turns; the excitation current: $i_e = \sin(2\pi 50t)$ A; $f = 50$ Hz; the parameters of the transformer with a closed toroidal core: $b_{(tr)} = 0{,}02\ m$; $h_{(tr)} = 0{,}02\ m$; $r_{mean.} = 0{,}05$ m; $\mu = 10^4$; $\mu_0 = 4\pi \cdot 10^{-7}\ H/m$; $w_{(tr).1} = w_{(tr).2} = 500$.

In the calculations, the magnetic reluctance of the steel part of the transducer magnetic core is neglected because it is much smaller than the magnetic reluctance of the working air gap. The fringing fluxes at the ends of the magnetic core and in the region of the transducer's moving element are also neglected.

The per-unit-length magnetic permeance of the working air gap between two adjacent elongated limbs is determined as follows:

$$G_{\mu wg} = \mu_0 \frac{b}{\delta_w} = 2{,}5 \cdot 10^{-6}\ H/m. \qquad (7)$$

The excitation magnetomotive force (MMF):

$$F_e = F_e + I_{em} w_e \sin \omega t = 100 + 100 \sin 314t. \qquad (8)$$

The working magnetic flux:

$$\Phi_w = 2 F_e G_{\mu wg} x = 5 \cdot 10^{-4} x + 5 \cdot 10^{-4} x \sin 314t. \qquad (9)$$

The EMF induced in the measuring winding as it moves along the central elongated limb, as determined from Eq. (2), is given by:

$$e_{meas} = w_{meas} \frac{d\Phi_w}{dt} = 5 \cdot 10^{-3} v + 1{,}57 x \cos 314t +$$

$$+5 \cdot 10^{-3} v \sin 314t = E_v + e_x + e_{gen.}. \qquad (10)$$

Next, we calculate the resistance and inductive reactance of the measuring winding and the primary winding of the transformer. For these windings, a copper wire with a diameter of $d = 0{,}4$ mm and a per-unit-length resistance of $R_l = 0{,}14\ Om/m$ [11]. is selected.

$R_{L.meas} = R_l l_{meas} = 0{,}14 \cdot 0{,}8 = 0{,}112\ Om$ (l_{meas} –the total length of the wire of the measuring winding for $w_{meas} = 10$ turns.

$R_{L.tr.1} = R_{L.tr.2} = R_l l_{tr.1} = 0{,}14 \cdot 24 = 3{,}36\ Om$ ($l_{tr.1}$ –the total length of the wire of the transformer's primary winding for $w_{tr.1} = 500$ turns.

$L_{meas} = 2 w_{meas}^2 G_{\mu wg} x = 5 \cdot 10^{-4} x$ H.

$L_{1(tr)} = L_{2(tr)} = w_{tr.1}^2 G_{\mu tr.} = w_{tr.1}^2\ \mu \mu_0 \frac{b_{tr} h_{tr}}{2\pi r_{mean.}} = 1{,}0$ H.

$X_{L.meas} = \omega L_{meas} = 0{,}157x$ H.

$X_{L_1(tr)} = \omega L_{1(tr)} = 314$ Om;

We assume that the transformer is ideal [10], i.e., $M_{12} = L_{1(tr)} = L_{2(tr)} = 1{,}0\ H$, where M_{12} is the mutual inductance between the primary and secondary windings of the transformer.

The capacitance of the capacitor is determined from the condition that the load current reaches its maximum value, at which the output signal proportional to the displacement of the moving winding is also maximized. For the specified values of e_{meas}, $R_{L.meas}$, $R_{L.tr.1}$, $X_{L.meas}$ and $X_{L_1(tr)}$ the load current attains its maximum value when the following voltage resonance condition is satisfied in the measuring circuit:

$$X_{L_1(tr)} = X_C. \qquad (11)$$

hence, we obtain:

$$C = \frac{1}{\omega X_{L_1(tr)}} = 1{,}01424 \cdot 10^{-5}\ \text{F}.$$

$$X_C = \frac{1}{\omega C} \approx 314\ \text{m}.$$

The complex representation of the alternating component of the EMF induced in the moving measuring winding can be written as follows:

$$\dot{E}_{meas.(\sim)} = \dot{E}_x + \dot{E}_{gen.} = j1{,}57x + 5 \cdot 10^{-3} v. \qquad (12)$$

Considering that the velocity of the moving element under dynamic operating conditions varies from 0 to 0,1 m/s [6,7], while the displacement range of the moving winding is 0 to 0,1 m, the component $\dot{E}_{gen.}$ can be neglected in Eq. (12), since its magnitude is insignificant compared with $\dot{E}_x$.

Substituting Eqs. (11) and (12) into Eq. (4), the load current is obtained as follows:

$$\dot{I}_l = \frac{j1{,}57x}{\sqrt{2}(3{,}472 + j0{,}157x\,)}. \qquad (13)$$

The reactance $X_{L.meas}$ reaches its maximum value at $x = X_{\text{M}} = 0{,}1\ m$ and is equal to $0{,}0157\ om$. Since $3{,}472 \gg 0{,}0157$ om, the magnitude of the load current can be expressed as:

$$I_l \approx \frac{1{,}57x}{\sqrt{2}}, \text{A}. \qquad (14)$$

The output signal proportional to the displacement of the moving winding, taken from the secondary winding of the transformer, is determined from Eq. (10) as follows:

$$E_{out.(x)} = \omega M_{12} I_l = \frac{493x}{\sqrt{2}}, \text{V}. \qquad (15)$$

The output signal of the existing transducer, proportional to the velocity of the moving measuring winding and taken from the terminals of the capacitor, is determined as follows:

$$\dot{U}_{out.(v)} = E_v - jX_C \dot{I}_l = 5 \cdot 10^{-3} v + \frac{493x}{\sqrt{2}}.. \qquad (16)$$

The displacement sensitivity of the existing motion parameter transducer, calculated using Eq. (6), is given by:

$$S_{(x)} = \frac{dE_{out.x}}{dx} = \frac{493}{\sqrt{2}}, \qquad (17)$$

A transformer resonant motion parameter transducer (TRMPS) was developed at the Department of Electrical Power Supply of Tashkent State Transport University (Fig. 3) [12].

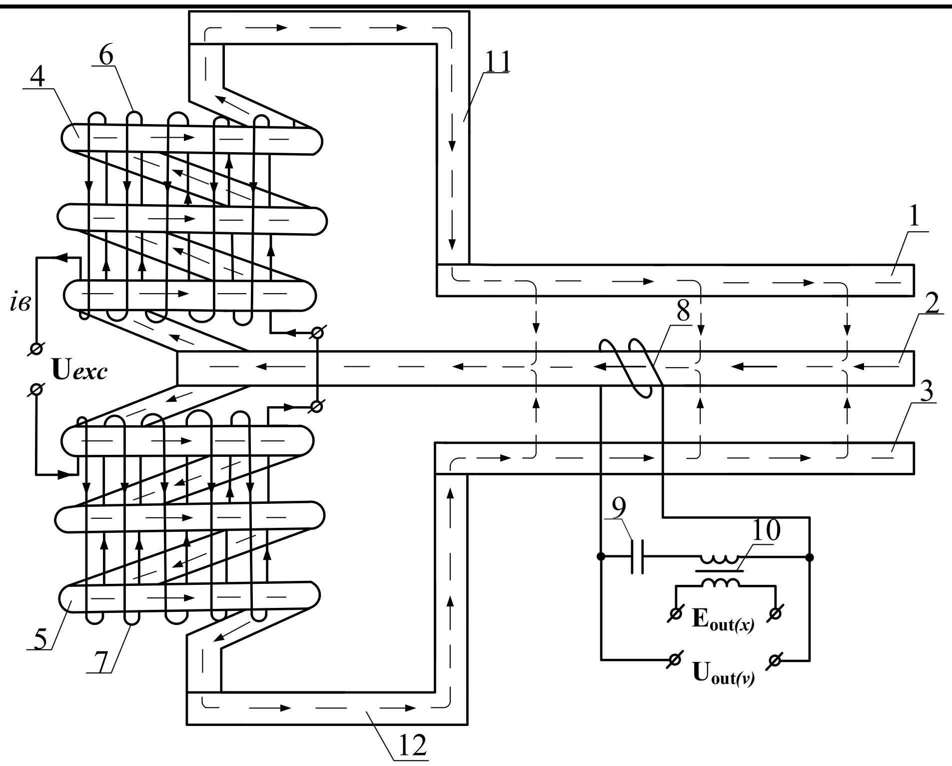

Fig. 3. Structural diagram of the proposed transformer resonant motion parameter transducer (TRMPS).

The proposed motion parameter transducer consists of a magnetic core formed by three elongated parallel limbs (1, 2, and 3). At the base of the core, two magnetic field sources are installed, each implemented as a multi-turn magnetic core (4 and 5) with corresponding sections of the excitation winding (6 and 7). These winding sections are connected so that their magnetic fluxes are oppositely directed and combine in the central limb (2). A concentrated moving measuring winding (8), mounted on the central limb of the magnetic core and mechanically coupled to the monitored object, is connected in series with a capacitor (9) and

the primary winding of a transformer (10). The capacitor and the transformer's primary winding are tuned to the voltage resonance condition.

To reduce the working air gaps between adjacent elongated limbs, ferromagnetic bridges (11 and 12) are employed. Each bridge connects the end portion of the corresponding outer limb to the respective end of the multi-turn magnetic core.

The excitation winding is supplied from a voltage source with an output voltage of

$u_e = U_{e.0} + U_{e.m} sin\omega t$, where $U_{e.0}$ is the DC component, while $U_{e.m}$ and ω are the amplitude and angular frequency of the sinusoidal excitation voltage, respectively.

The circuit parameters are selected such that the inductive reactance of the transformer's primary winding is much greater than its resistance, i.e., $X_{L_1(tr)} \gg R_{L_1(tr)}$. Therefore, the resistance of the primary winding can be neglected, and $R_{L_1(tr)} \approx 0$.

The output signal proportional to the magnitude and direction of displacement is taken from the secondary winding of the transformer, whereas the output signal proportional to the displacement velocity is taken from the output terminals of the measuring winding.

The motion parameter transducer operates as follows. The excitation winding is supplied from a power source with a voltage $u_e = U_{e.0} + U_{e.m} sin\omega t$. Under the action of this voltage, the excitation circuit carries a current $i_e = I_{e.0} + I_{e.m} sin(\omega t + \varphi_e)$, where φ_e is the phase angle between the alternating components of the excitation voltage and current.

As this current flows through the turns of the excitation winding sections, each turn of the multi-turn magnetic core generates a magnetomotive force (MMF), the magnitude of which is determined by the following expression:

$$F_e = F_{e.0} + F_{e.m} sin(\omega t + \varphi_e) = w_0 I_{e.0} + w_0 I_{e.m} sin(\omega t + \varphi_e), \quad (18)$$

here $F_{e.0} = w_0 I_{e.0}$ и $F_{e.m} = w_0 I_{e.m}$ – the DC and AC components of the magnetomotive force (MMF) in each turn of the multi-turn magnetic core, produced by the DC and AC components of the excitation current, respectively; w_0 – the number of turns in one section of the excitation winding;

The total magnetomotive force (MMF) at the terminals of the multi-turn magnetic core of each magnetic field source is determined as the arithmetic sum of the MMFs generated in all turns of the multi-turn magnetic core, i.e.:

$$F_{e\Sigma} = F_{e.0.\Sigma} + F_{e.m.\Sigma} sin(\omega t + \varphi_e) = w_{m.c} w_0 I_{e.0} + w_{m.c} w_0 I_{e.m} sin(\omega t + \varphi_e) \quad (19)$$

here $w_{m.c}$ – is the number of turns in the multi-turn magnetic core. It should be noted that, in deriving Eq. (19), the active and reactive magnetic reluctances of the multi-turn magnetic core are neglected in the first approximation because they are much smaller than the magnetic reluctances of the working air gaps between the corresponding elongated limbs of the magnetic core.

When the moving measuring winding (8) is displaced, an electromotive force (EMF) is induced in it according to the law of electromagnetic induction. The induced EMF is determined by the following expression:

$$e_{meas} = 2w_{meas} \frac{d\Phi_e}{dt} = E_v + e_x + e_v = 2w_{m.c} w_0 w_{meas} I_{e.0} G_{\mu wg} v +$$
$$2\omega w_{m.c} w_0 w_{meas} \cdot\cdot I_{e.m} G_{\mu wg} x cos(\omega t + \varphi_e) +$$
$$2w_{\text{м}} w_0 w_{meas} I_{e.m} G_{\mu wg} v sin(\omega t + \varphi_e), \quad (20)$$

A comparative analysis of Eqs. (2) and (20) shows that the EMF induced in the measuring winding of the proposed transformer resonant motion parameter transducer (TRMPS) during its displacement is $w_{m.c}$ times greater than the corresponding EMF induced in the existing transformer resonant motion parameter transducer.

For the same geometric dimensions, parameters, and assumptions adopted above, the DC component and the complex value of the AC component of the EMF

induced in the moving measuring winding of the proposed transducer are respectively given by:

$$E_v = 2w_{m.c}w_0w_{meas}I_{e.0}G_{\mu wg}v = 5 \cdot 10^{-3}w_{m.c}v, \qquad (21)$$

$$\dot{E}_{meas.(\sim)} = j2\omega w_{m.c}w_0I_{e.m}G_{\mu wg}x = j1{,}57w_{m.c}x. \qquad (22)$$

The load current is given by:

$$I_l \approx \frac{1{,}57w_{m.c}x}{\sqrt{2}}, \text{ A.} \qquad (23)$$

Since the load, consisting of the capacitor (9) connected in series with the primary winding of the transformer (10), is tuned to the voltage resonance condition ($X_{L_1(\text{тр})} = X_C$), the expression for $\dot{U}_{\text{вых.}(v)}$ takes the following form:

$$\dot{U}_{out.(v)} = E_v + \dot{I}_lR_{L_1(tr)}. \qquad (24)$$

For the same geometric dimensions, parameters, and assumptions adopted above, the useful output signals of the proposed transducer, proportional to the displacement and its velocity, as well as the corresponding sensitivity, are given by:

$$E_{out.(x)} = \omega M_{12}I_l = \frac{493w_{m.c}x}{\sqrt{2}}, \text{ V.} \qquad (25)$$

$$\dot{U}_{out.(v)} = E_v + \dot{I}_lR_{L_1(tr)} = 5 \cdot 10^{-3}w_{m.c}v + \frac{5{,}28w_{m.c}x}{\sqrt{2}}, \text{ V.} \qquad (26)$$

$$S_{(x)} = \frac{dE_{out..x}}{dx} = \frac{493w_{m.c}}{\sqrt{2}}, \qquad (27)$$

Thus, a comparative analysis of the derived expressions for the output signals and sensitivities of the conventional and proposed transformer resonant motion parameter transducers demonstrates that the sensitivity of the proposed transducer is $w_{m.c}$ times higher than that of the conventional transducer, where $w_{m.c}$ is the number of turns in the multi-turn magnetic core. This improvement is achieved by implementing each magnetic field source as a multi-turn magnetic core with an excitation winding section whose turns encompass all turns of the multi-turn magnetic core. In addition, the proposed transducer provides higher accuracy in measuring the velocity of the moving winding (the monitored object) by minimizing the amplitude of the AC component of the output signal that is not proportional to the displacement velocity. This is accomplished by extracting the velocity-proportional signal directly from the terminals of the moving measuring winding, while the load circuit is tuned to the voltage resonance condition.

References

[1] N.R. Yusupbekov, Kh.Z. Igamberdiev, and A.V. Malikov, *Fundamentals of Automation of Technological Processes: A Textbook for Higher and Secondary Specialized Education*, Parts 1–2 (Tashkent State Technical University, Tashkent, Uzbekistan, 2007), 152 p., 173 p.

[2] I.V. Miroshnik, *Theory of Automatic Control: Linear Systems* (Piter Publishing House, St. Petersburg, Russia, 2005), 336 p.

[3] M.Yu. Rachkov, *Technical Means of Automation: A Textbook for Higher Education* (Moscow State Industrial University, Moscow, Russia, 2006), 185 p.

[4] V.G. Lukashkin, V.K. Garipov, V.V. Sleptsov, and A.V. Vishnekov, *Automation of Measurement, Control and Management* (Mashinostroenie, Moscow, Russia, 2005), 663 p.

[5] A.V. Fedotov, *Theory and Design of Inductive Displacement Transducers for Automatic Control Systems* (Omsk State Technical University Press, Omsk, Russia, 2011), 176 p.

[6] N.E. Konyukhov, F.M. Mednikov, and M.L. Nechaevskii, *Electromagnetic Transducers of Mechanical Quantities* (Mashinostroenie, Moscow, Russia, 1987), 256 p.

[7] M.F. Zaripov, *Transducers with Distributed Parameters for Automation and Information-Measuring Technology* (Energiya Publishing House, Moscow, Russia, 1969), 176 p.

[8] S. Amirov, A. Sulliev, A. Sanbetova, and I. Kurbonov, "Study on the Biparametric Transduction Circuits with Distributed Parameters," *IOP Conference Series: Earth and Environmental Science*, 939, Proceedings of the 2nd International Conference on Energetics, Civil and Agricultural Engineering (ICECAE 2021), 14–16 October 2021.

[9] M.F. Zaripov, S.F. Rakhmatulin, N.A. Bogdanova, and M.V. Belyaev, "Motion Parameter Transducer," USSR Author's Certificate No. 448385, *Official Bulletin*, no. 40, 1974.

[10] K.S. Demirchyan, L.R. Neyman, N.V. Korovkin, and V.L. Chechurin, *Theoretical Foundations of Electrical Engineering*, 4th ed., Vol. 1 (Piter Publishing House, St. Petersburg, Russia, 2006), 464 p.

[11] F.F. Karpov, *Handbook for the Design of Wires and Cables* (Moscow, Russia, 2019), 488 p.

[12] S.F. Amirov, A.Kh. Sulliev, S.A. Norjigitov, J.S. Fayzullaev, and U.B. Mukhtorov, *Motion Parameter Transducer*, Patent Application of the Republic of Uzbekistan No. IAP 2023 0413, filed July 25, 2023.